



GASTROINTESTINAL, HEPATOBILIARY, AND PANCREATIC PATHOLOGY

Chronic Intestinal Inflammation Suppresses Brain Activity by Inducing Neuroinflammation in Mice



Jonathon Mitchell,* Su Jin Kim,*[†] Cody Howe,* Seulah Lee,[†] Ji Yun Her,[†] Marisa Patel,* Gayoung Kim,* Jaewon Lee,[†] Eunok Im,[†] and Sang Hoon Rhee*[†]

From the Department of Biological Sciences,* Oakland University, Rochester, Michigan; and the College of Pharmacy,[†] Pusan National University, Busan, Republic of Korea

Accepted for publication
September 22, 2021.

Address correspondence to
Sang Hoon Rhee, Ph.D.,
Department of Biological Sci-
ences, Oakland University, 330
Dodge Hall, 118 Library Dr.,
Rochester, MI 48309; and
Eunok Im, Ph.D., College of
Pharmacy, Pusan National
University, 2, Busandaehak-ro
63beon-gil, Bldg., 503, Room
801, Geumjeong-gu, Busan,
46241, South Korea. E-mail:
srhee@oakland.edu and eoim@pusan.ac.kr.

Chronic gut inflammation such as inflammatory bowel disease is believed to be associated with neurodegenerative diseases in humans. However, the direct evidence for and the underlying mechanism of this brain–gut interaction remain elusive. In this study, manganese-enhanced magnetic resonance imaging was used to assess functional brain activity from awake and freely moving mice with chronic colitis. Manganese ion uptake (indicative of Ca²⁺ influx into neuronal cells) and accumulation were reduced in the hippocampus of chronic colitis mice compared with control mice. Long-term memory declined and neuroinflammatory signals, including IL-1 β production and activation of caspase-1, caspase-11, and gasdermin, were induced. High-mobility group box 1 (HMGB1) levels were elevated both in the serum and in the hippocampus; however, lipopolysaccharide (LPS) levels remained at low levels without significant changes in these samples. The blood–brain barrier permeability was increased in chronic colitis mice. In the presence of LPS, HMGB1 treatment induced the activation of caspase-11 and gasdermin in the mouse microglial cell line SIM-A9. These findings suggest that HMGB1 released from the inflamed intestine may move to the brain through the blood circulatory system; in conjunction with a low level of endogenous LPS, elevated HMGB1 can subsequently activate caspase-mediated inflammatory responses in the brain. (*Am J Pathol* 2022, 192: 72–86; <https://doi.org/10.1016/j.ajpath.2021.09.006>)

Although the gut and brain are separated anatomically, emerging evidence implies that these organs communicate and influence each other's physiological functioning in a bidirectional manner.¹ In case of the descending pathway of the gut–brain axis, psychological stress is believed to play a prominent role in the development and progression of irritable bowel syndrome and also may increase the risk of inflammatory bowel diseases (IBDs).^{2,3} Specifically, the brain–gut interaction may contribute to an increased risk of IBD such as in Crohn's disease (CD) and ulcerative colitis, because psychological stress might increase intestinal permeability, thereby allowing luminal constituents access to the submucosal immune system, leading to intestinal inflammation.⁴ In case of the ascending pathway of the gut–brain axis, signals from the intestine are thought to influence brain physiology. A recent study suggested that the healthy

human appendix contains α -synuclein aggregates that accumulate in Lewy bodies of Parkinson disease; accordingly, appendectomy may lower the risk of Parkinson disease in humans.⁵ This study supports the notion that intestinal physiology is linked to a brain disorder. Furthermore, patients with gut inflammatory disorders such as celiac disease^{6,7} and IBD⁸ experience transient cognitive impairments called *brain fog* manifested by memory issues, disorientation, hazy thought processes, and slow cognitive reaction time.⁷ Patients with IBD may also experience psychological disorders.^{9,10} These studies imply that chronic intestinal inflammation can influence brain

Supported by NIH grant DK125941 (S.H.R.) and Korean government (MSIT) grant 2019R1A2C1010536 (E.I.).

J.M. and S.J.K. contributed equally to this work.

functionality. Likewise, another study suggested that the mRNA levels of pro-IL-1 β and tumor necrosis factor α were higher in the hippocampus of multi-cycle dextran sulfate sodium (DSS)-treated mice than in healthy mice.¹¹ However, whether intestinal inflammation elicits a pathologic condition in the brain is still unknown.

Magnetic resonance imaging (MRI) is an excellent noninvasive imaging technique to visualize the anatomic structure and function of soft tissues in living organisms.¹² Among the variety of MRI approaches, the use of the manganese ion as a contrast agent has been developed as the manganese-enhanced MRI (MEMRI) for studying *in vivo* brain activity.¹³ Ca²⁺ is a crucial intracellular second messenger required for mediating neuronal cell signaling in the brain. Depolarization of neurons increases the concentration of Ca²⁺ in the cytoplasm because it enters cells through L-type Ca²⁺ channels.¹⁴ Nontoxic levels of the paramagnetic Mn²⁺ ion also enter cells via L-type Ca²⁺ channels and accumulate inside the cell.¹⁵ MEMRI was developed to sensitize MRI to qualitatively monitor calcium influx in the brains of rodents.¹⁵ Therefore, systemic administration of Mn²⁺ *in vivo* confers contrast that encodes neuronal activity.

The present study used MEMRI to examine the brain activity of living mice with chronic colitis induced by multi-cycle DSS treatment. It further investigated the mechanism by which chronic intestinal inflammation could change brain physiology.

Materials and Methods

Animals

C57BL/6 mice and CD-1 mice were purchased from The Jackson Laboratory (Bar Harbor, ME) and Charles River Laboratories (Wilmington, MA), respectively. All animal experiments were approved by the Institutional Animal Care and Use Committees (IACUC) of Oakland University (IACUC-16122; Rochester, MI), Wayne State University (IACUC-18-02-0555; Detroit, MI), and Pusan National University (IACUC number PNU-2018-1843; Busan, Republic of Korea). Mice were bred and maintained in a specific pathogen-free condition with normal drinking water *ad libitum* at the AAALAC-accredited animal facility under the approval of the IACUC.

Chronic Colitis Mouse Model

DSS (mol. wt. 40,000-50,000) was purchased from Affymetrix, Inc. (Cleveland, OH). Three-cycle DSS treatment has been used as a mouse model of chronic colitis.^{11,16} Age-matched (8 weeks old) and sex-matched C57BL/6 mice were randomly selected for the experiment. Mice were orally treated with 2.5% DSS (w/v)-laced water for 5 days to induce colitis. They were then treated with normal drinking water for 6 days for recovery. Mice were treated with three

cycles of DSS and subsequent normal drinking water for a total of 28 days. For the healthy control group, mice were treated with regular drinking water throughout the experimental period.¹⁷

Mouse MEMRI

Randomly selected male mice (8 weeks old; $n = 8$ per group) were treated with three cycles of DSS or regular water to prepare chronic colitis or healthy control mice. After completing the third cycle of DSS treatment, mice were given an i.p. injection of MnCl₂ (66 mg/kg) and were placed in a normal housing condition. Four hours after this injection, mice were anesthetized by using isoflurane, and MRI data were acquired on a 7T Bruker Scanner 70/30 MRI system (Bruker ClinScan; Bruker Corporation, Billerica, MA). Mouse brain T1 data were acquired by using a dual coil mode on a 7T Bruker system, as previously described.^{18,19} Several single spin-echo (time to echo, 13 ms; matrix size, 160 \times 320; and slice thickness, 600 μ m) images were acquired at different repetition times. To compensate for reduced signal-noise ratios at shorter repetition times, progressively more images were collected as the repetition time decreased. A single slice was then collected, representing the same anatomic brain region in each mouse for comparison of the dorsal hippocampus. The mouse MEMRI procedure and the data analysis were performed in the MR Core Research Facility at Wayne State University in accordance with the protocol previously described.¹⁸

Blood-Brain Barrier Permeability Assay

Randomly selected, sex- and age-matched CD-1 mice were subjected to DSS-induced chronic colitis and healthy control mice. After finishing the third cycle of DSS treatment, mice (colitis, $n = 11$; control, $n = 7$) were tail vein injected with Evans blue dye (EBD; 2%) prepared in 0.9% NaCl saline.^{20,21} One hour after the injection, mice were anesthetized with isoflurane and transcardially perfused with saline solution until the perfusate from the right atrium ran clear. The brain was harvested and weighed. The brains were rinsed in saline and dried at 60°C for 48 hours. EBD was extracted by incubating the tissue in 0.5 mL of formamide at room temperature for 48 hours. EBD was quantified by using spectrofluorimetry (excitation, 620 nm; emission, 680 nm). Data were normalized according to the brain weight.

Passive Avoidance Test to Measure Memory Performance in Mice

The passive avoidance test is a classical protocol to assess memory performance in mice.²² It was conducted in a two-compartment box composed of a lighted and a dark compartment. Briefly, mice were placed in a lighted side

and offered access through a narrow gate to a closed dark compartment. When a mouse entered the dark room due to its natural instinct, the gate was closed, and an electric shock was delivered to the paw (0.25 mA, 3 seconds). During this training period, the mice learn that moving to the dark room confers a stressor (this phase of the test is termed the “training” or “learning” phase). After this training, the mice were taken to a home cage for routine housing.

One day after training, the mice were again placed in the lighted compartment, and the passive avoidance response was evaluated. The latency (time) to enter the dark compartment was used as a measurement of memory performance for up to 300 seconds.²³ The results from this test are regarded as a short-term memory measurement. These mice were returned to home cages and housed for an additional 7 days. They were once again placed in the lighted compartment for another test, and the latency to enter the dark compartment was similarly measured. The number of times the mice attempted to enter the dark room (entry attempts) were recorded. The latency of the first attempt to enter (first entry attempt) was also measured. These data are interpreted as a long-term memory measurement.

To minimize potential effects of hormonal variation, randomly selected male C57BL/6 mice (8 weeks old, $n = 21$ or 14 per group) were treated with three cycles of DSS or regular water to emulate chronic colitis. After finishing the third cycle of DSS-induced colitis, the mice were treated with water for 3 days for a brief recovery period before the test, followed by the passive avoidance test.

Gas Chromatography—Mass Spectrometry Analysis to Quantify Short-Chain Fatty Acids

Sample Preparation

The hippocampus and cerebrum tissues were isolated from the whole mouse brain. Then, 50 mg of each tissue was transferred to a pre-weighed locked Eppendorf tube, and 600 μ L of 30 mmol/L hydrochloric acid containing isotopically labeled acetate (150 μ mol/L), propionate (75 μ mol/L), butyrate, isobutyrate, valerate (30 μ mol/L), isovalerate, hexanoate, heptanoate, and octanoate (15 μ mol/L) was added to each sample. Samples were homogenized in a Bullet Blender Gold (Next Advance, Inc., Troy, NY) for 5 minutes at speed 8. Samples were vortexed for 10 seconds, incubated for 10 minutes on ice, and then vortexed again for 10 seconds. Samples were then centrifuged at $1500 \times g$ at 4°C for 10 minutes, and the supernatant was transferred to a 1 mL glass tube. Then, 20 μ L of each sample was removed to a separate glass vial to create a pooled sample for quality control purposes; 300 μ L of methyl tert-butyl ether was added to each sample and the mixture vortexed for 10 seconds to emulsify, then held at 4°C for 5 minutes and vortexed again for 10 seconds. Samples were centrifuged for 1 minute to separate the

solvent layers, and the methyl tert-butyl ether layer was then removed to an autosampler vial for gas chromatography—mass spectrometry (GC-MS) analysis. A series of calibration standards were prepared along with samples to quantify metabolites. Postextract, tissues were taken to dryness in SpeedVac (Thermo Fisher Scientific) and the Eppendorf tube re-weighed to obtain the dry tissue weight for normalization.

GC-MS Analysis

GC-MS analysis was performed on an Agilent 69890N GC-5973 MS detector (Santa Clara, CA) with the following parameters: a 1 μ L sample was injected with a 1:10 split ratio on a ZB-WAXplus, 30 m \times 0.25 mm \times 0.25 μ m (catalog number 7HG-G013-11; Phenomenex, Torrance, CA) GC column, with He as the carrier gas at a flow rate of 1.1 mL/min. The injector temperature was 240°C, and the column temperature was isocratic at 310°C.

Data Analysis

Data were processed by using MassHunter Quantitative analysis version B.07.00 (Agilent). Short-chain fatty acids were normalized to the nearest isotope-labeled internal standard and quantitated by using two replicated injections of five standards to create a linear calibration curve with accuracy better than 80% for each standard. Samples were normalized to dry sample weight after quantification.

Metabolomics Core Services at the University of Michigan (Ann Arbor, MI) were used for the GC-MS analysis in accordance with a previous study.²⁴

Cell Culture

A mouse microglial cell line, SIM-A9 cell (ATCC CRL-3265),²⁵ was purchased from ATCC (Manassas, VA) and cultivated with Dulbecco's Modified Eagle Medium/Nutrient Mixture F-12 supplemented with 10% heat-inactivated fetal bovine serum, 1% L-glutamine, penicillin (100 IU/mL), and streptomycin (100 μ g/mL) at 37°C in a 5% carbon dioxide air environment. Mouse HMGB1 protein from ACRO Biosystems (Newark, DE) and lipopolysaccharide (LPS) from InvivoGen (San Diego, CA) were used to stimulate the cells.

Immunofluorescence Staining of the Mouse Brain Tissue Sections

To prepare mouse brain tissues for immunofluorescence staining, mice were anesthetized by using isoflurane and subjected to a transcardial perfusion fixation procedure using 0.9% NaCl in phosphate-buffered saline (PBS) (pH 7.4) and 4% paraformaldehyde solution perfused through the circulatory system to rapidly and uniformly preserve the intact brain tissue. Harvested brain tissues were preserved in 4% paraformaldehyde solution at 4°C overnight. Fixed

tissues were rinsed three times with fresh PBS and stored in 30% sucrose solution in PBS until the tissue sinks. Prepared tissues were embedded in paraffin block and sectioned at 8 μ m thickness.

The slides with tissue sections were dewaxed with xylene for 7 minutes twice and rehydrated with 100% ethanol for 2 minutes twice. Sections were soaked in 95% ethanol for 2 minutes and then 70% ethanol for 2 minutes. Those were rinsed with distilled water and boiled in sodium citrate buffer at 95°C to 99°C for 20 minutes to antigen retrieval. Slides were washed with TBS-T (tris-buffered saline, 0.1% tween 20) for 5 minutes twice and rinsed with distilled water. To reduce surface tension, tissues were washed with PBS containing 0.05% Triton X-100 for 5 minutes twice. Sections were soaked in blocking buffer Protein Block, Serum-Free (Agilent), containing 0.1% Triton X-100 to block nonspecific binding for 2 hours at room temperature. Primary antibody [glial fibrillary acidic protein (GFAP) monoclonal antibody, MA5-12023, from Thermo Fisher Scientific (Waltham, MA) or IL-1 β antibody, ab9722, from Abcam (Cambridge, UK)] was diluted in blocking buffer in a 1:200 ratio. Slides containing blocked tissues were incubated in a humidified chamber, 4°C overnight. After incubation, slides were soaked in PBS-T (phosphate-buffered saline, 0.1% tween 20) for 5 minutes, and the process repeated four times. The secondary antibodies, goat anti-mouse IgG-heavy and light chain Antibody DyLight594 Conjugated (A90-138D4) for GFAP antibody and goat anti-Rabbit IgG-heavy and light chain Antibody FITC Conjugated (A120-101F) for IL-1 β antibody, were from Bethyl Laboratory, Inc. (Montgomery, TX).

After preparing diluted secondary antibodies with blocking buffer, the secondary antibody was added to slides and incubated for 2 hours at room temperature. Slides were rinsed thoroughly five times with PBS-T, 5 minutes each. For the GFAP and IL-1 β staining, the slides were mounted with VECTASHIELD Mounting Medium with DAPI (Vector Laboratories, Burlingame, CA). Stained tissues were observed by using a Zeiss LSM 800 confocal microscope, and confocal images were analyzed by using Zen 2 software (Carl Zeiss AG, Oberkochen, Germany).

Enzyme-Linked Immunosorbent Assay Quantification of IL-1 β , IL-6, and High-Mobility Group Box 1

We used enzyme-linked immunosorbent assay (ELISA) kits (mouse IL-6 and IL-1 β) compatible with the tissue extract samples, which are from RayBiotech Inc. (Norcross, GA). The mouse high-mobility group box 1 (HMGB1) ELISA kit was acquired from LSBio (Seattle, WA). The hippocampus and cerebrum tissues were homogenized in radio-immunoprecipitation assay lysis buffer supplemented with cOmplete Protease Inhibitor Cocktail and Phosphatase Inhibitor Cocktail 2 and 3 (MilliporeSigma, St. Louis, MO), followed by evaluation of the total protein concentration using the Pierce BCA Protein Assay Kit (Thermo Fisher

Scientific). Blood samples were collected from mice by cardiac puncture. The samples were placed in CAPIJECT Micro Collection Tubes (T-MG, Terumo Medical Corporation, Somerset, NJ) containing a clot activator and allowed to clot over 45 minutes at room temperature. Serum samples were prepared by centrifugation at 1500 \times g. ELISA was performed in accordance with the manufacturer's instruction. The concentration was normalized according to the total protein concentration of the sample. All assays were performed in triplicate, and data are shown as means \pm SEM.

Endotoxin Quantification

The brain tissue lysate was prepared by using radio-immunoprecipitation assay buffer containing cOmplete EDTA-Free Protease Inhibitor Cocktail, Phosphatase Inhibitor Cocktail 2 and 3. The mouse blood serum was collected in CAPIJECT Micro Collection Tubes and incubated 45 minutes at room temperature to clot. Serum was separated by centrifugation. For this assay, all materials, including sample tubes, pipette tips, serologic pipette, disposable 96-well plates, and eight-strip PCR tubes, were prepared as endotoxin free. In case of brain tissue lysate, all protein concentrations were adjusted to 1 μ g/mL with endotoxin-free water. In case of mouse serum, a sample was diluted with endotoxin-free water at a 1:100 ratio. The brain tissue lysate and mouse blood serum samples were used to quantitate endotoxin LPS with a Pierce Chromogenic Endotoxin Quant Kit (88282; Thermo Fisher Scientific) in accordance with the manufacturer's instructions.

Because it is important to maintain the correct temperature at 37°C throughout the assay procedure, we used a thermocycler PCR machine during the assay procedure. Before starting this assay, the PCR machine and tubes were sufficiently preheated. Together with the standard solution of endotoxin, the tissue lysate or serum samples (50 μ L) were added in PCR tubes in triplicate. Then, the reconstituted amebocyte lysate reagent (50 μ L) was added to the PCR tubes and gently mixed. After incubation at 37°C for 10 minutes, prewarmed (37°C) chromogenic substrate solution (100 μ L) was added to each tube and gently mixed again, followed by incubation at 37°C for 6 minutes. Then, 50 μ L of Stop Solution (25% acetic acid) was added to each tube. The optical density at 405 nm was then measured.

The endotoxin concentration [endotoxin units per milliliter (EU/mL)] was determined by plotting a standard curve; the standard range was 0 EU/mL to 1.0 EU/mL. In cases of brain tissue lysate samples, we recalculated endotoxin concentration with protein amount and presented the concentration of relative endotoxin (EU per milligram). In cases of mouse blood serum samples, a dilution factor (100) was applied to all values, and a recalculated endotoxin concentration (EU/mL) was presented.

Immunoblot Analysis

After harvesting the whole brain from mice, the hippocampus and cerebrum tissues were separated. The tissues were then homogenized in the radioimmunoprecipitation assay lysis buffer supplemented with cOmplete Protease Inhibitor Cocktail and Phosphatase Inhibitor Cocktail 2 and 3. Total protein concentration was determined by using the Pierce BCA Protein Assay Kit. Equal amounts of total protein were mixed with Laemmli Sample Loading Buffer (Bio-Rad, Hercules, CA). To avoid the protein aggregation that usually occurs in the standard Western blotting procedure, the heat denaturation (boiling) step was omitted in this Western blot approach.^{26,27} SDS-PAGE analysis and immunoblotting were performed in accordance with a previous protocol²⁸ using antibodies that recognize caspase-1p20 (D-4, sc-398715), caspase-11p20 (A-2, sc-374615), and gasdermin (H-6, sc-376318) obtained from Santa Cruz Biotechnology (Dallas, TX), IL-10 antibody (RP1015) from Boster Biological Technology (Pleasanton, CA), and beta-actin antibody (8H10D10, #3700) from Cell Signaling Technology (Danvers, MA). Horseradish peroxidase-conjugated goat anti-mouse IgG secondary antibody or horseradish peroxidase-conjugated goat anti-rabbit IgG secondary antibody from Thermo Fisher Scientific was used at a dilution of 1:40,000 for at least 30 minutes.

Statistical Analysis

Data of body weight change were compared by using a two-way analysis of variance, followed by the multiple-comparison Bonferroni *t*-test to assess differences between groups.²⁹ Results are provided as means \pm SD. $P < 0.05$ was considered significant. Additional information regarding statistical analysis is described in the corresponding figure legends. Statistical analysis was conducted with GraphPad Prism 5 (GraphPad Software, Inc., San Diego, CA).

Results

Chronic Colitis Reduces *in Vivo* Brain Activity in Living Mice

DSS-induced colitis is an animal model of IBD that can easily emulate acute, chronic, or relapsing colitis by the oral administration of DSS.³⁰ As an experimental model of chronic colitis,^{11,16} C57BL/6 mice were treated with three cycles of DSS and intervening normal drinking water. DSS treatment resulted in marked weight loss, whereas water treatment led to recovery manifested by partial restoration of body weight (Supplemental Figure 1A). After three cycles of DSS treatment, the mouse colon was inflamed and much shorter in the DSS-treated mice than in the water-treated control mice (Supplemental Figure 1B). Histologic

sections of the colons from DSS-treated mice were characterized by destructive inflammation of the mucosa, manifested by massive neutrophil infiltration and epithelial damage. However, control mouse colons maintained an intact epithelium and normal mucosa (Supplemental Figure 1C). Thus, the multi-cycle DSS treatment was harnessed as a mouse model of chronic colitis.

Next, the MEMRI technique was used to examine the brain activity of living mice with chronic colitis. With 1/T1 mapping, it is possible to quantify soft tissue manganese uptake in MRI images, in which greater manganese uptake is manifested by brighter regions.¹⁸ Therefore, a series of T1 maps were acquired in which coronal brain slices depict brain anatomy and differential MEMRI signals depending on neuronal activity. The contrast enhancement of the brain anatomy revealed excellent cytoarchitectonic details of the neuroarchitecture due to the presence of Mn²⁺ in regions such as the hippocampus (Figure 1A).

To analyze manganese uptake, which is a proxy for brain activity, T1 images were converted into pseudo-color spin-lattice relaxation rate (1/T1) parameter maps, in which various levels of manganese were illustrated in correspondingly different colors (Figure 1B). Qualitative and quantitative analyses of 1/T1 parameter maps indicated that colitis mice had markedly lower manganese uptake ($P < 0.01$) in the hippocampus than in the same region of healthy mice (Figure 1, C and D).

Together, these results suggest that brain activity was reduced in chronic colitis mice compared with that of control mice.

Long-Term Memory Is Reduced in Chronic Colitis Mice

Given the MEMRI data, we hypothesized that chronic colitis would attenuate memory performance in mice. The passive avoidance test, a fear-motivated test that assesses short- and long-term memory, was conducted to test this hypothesis.²² Mice were placed in the lighted compartment (Figure 2A). A mouse entering the dark side triggered an electric shock to the paw. After this training, the mouse was again placed in the lighted compartment to measure memory (Figure 2B).

To perform this test, C57BL/6 mice were treated with three cycles of DSS or regular water (Figure 2C). After finishing the third cycle of DSS-induced colitis, mice were treated with regular water for 3 days for a brief recovery before the test. At the day 1 time point, most mice were reluctant to enter the dark room and thus appeared to have an intact memory of the distress that they had experienced in the dark chamber. Therefore, the passive avoidance test results were similar between the mouse groups. At the day 8 time point, however, the chronic colitis mice had a reduced latency of entry ($P < 0.05$) (Figure 2D) and more frequently attempted to enter the dark room ($P < 0.01$) (Figure 2E) compared with the healthy mice. Moreover, the colitis mice made their first attempt to enter the dark room much earlier

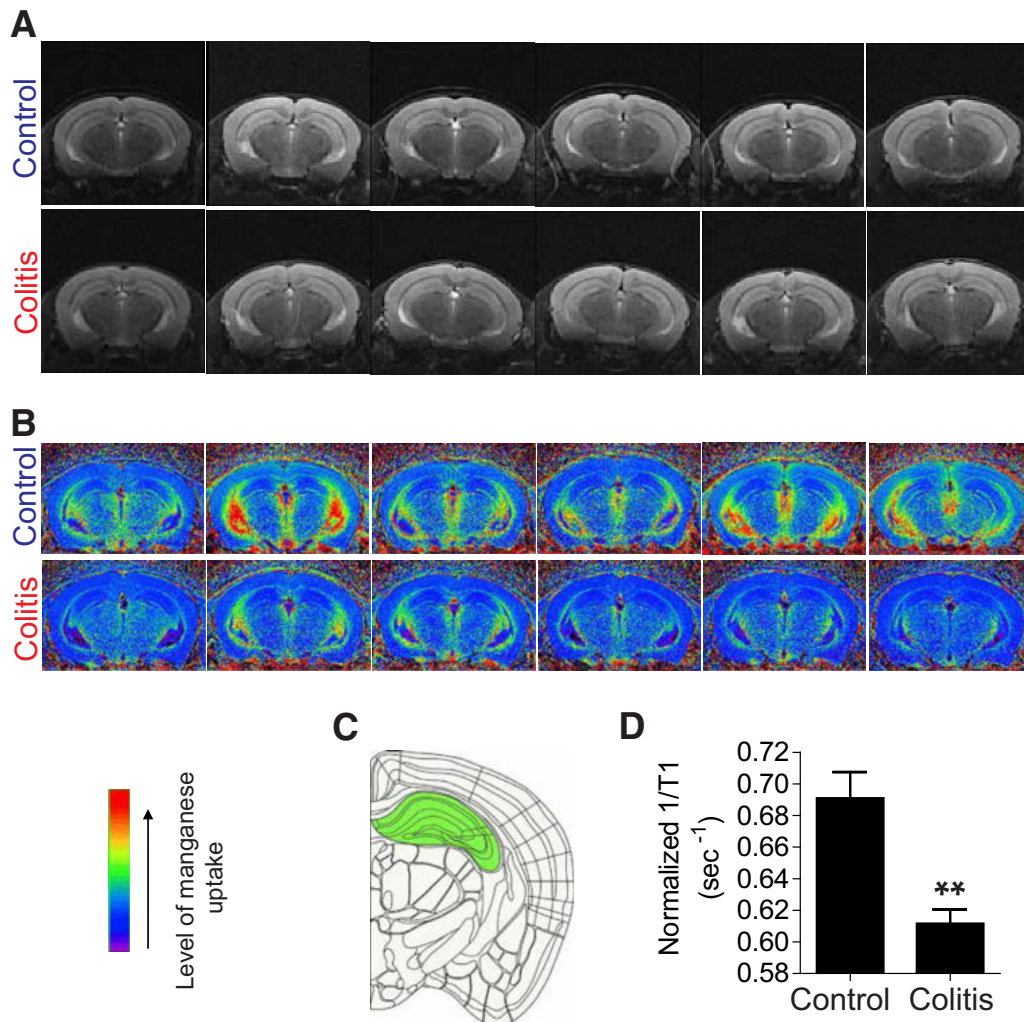


Figure 1 Brain activity examined by manganese-enhanced magnetic resonance imaging (MEMRI) is markedly reduced in the hippocampus of chronic colitis mice. To minimize any potential effects in the brain that may be hormonal or sex-based in nature, male C57BL/6 mice were used for the MEMRI experiment. **A:** Through the MEMRI technique, coronal MRI views of the mouse brain were acquired from coronal brain slices, and T1-weighted MRI of the mouse brain was generated. Among a series of slices, a single slice representing the same anatomic region was collected for comparison between colitis mouse brain and controls. Six representative T1-weighted MRI images are presented from a total of eight mice per group. **B:** The same slice of T1-weight images was converted into a pseudo-color spin-lattice relaxation rate (1/T1) parameter map, which illustrates differential levels of manganese uptake in the mouse brain. **C:** The hippocampus (green) is the region of interest that was analyzed to calculate the 1/T1 map. **D:** Manganese uptake in the hippocampus was quantitated by analyzing the color intensity in this brain region, as previously described.¹⁸ The reciprocal (1/T1) values directly reflect manganese levels, as the shortening of the T1 relaxation time depends on the variation of Mn²⁺ concentration.¹⁹ The error bars represent SDs. *n* = 8 per group. ***P* < 0.01 versus control (*U*-test).

than the healthy mice at the day 8 time point (*P* < 0.01) (Figure 2F).

These data suggest that long-term memory may have declined in the chronic colitis mice compared with the healthy control mice, whereas short-term memory was not changed.

Reactive Astrocytes Are Induced in the Brain of Chronic Colitis Mice

Astrocytes are a critical cell type in the brain and play a key role in maintaining homeostasis of the central nervous system.³¹ The activation of astrocytes results in the generation of reactive astrocytes that are characterized by

morphologic changes and the up-regulation of GFAP.³² Reactive astrocytes are observed in a variety of neuropathologies, including neuroinflammation, Parkinson disease, and Alzheimer disease.³³ Therefore, we hypothesized that chronic colitis mice might exhibit astrocyte activation in the brain. GFAP immunofluorescence staining of GFAP was performed to test this hypothesis.

The expression of GFAP was increased in the hippocampal brain region of the chronic colitis mice compared with the same region in the control mice (Figure 3A). Moreover, astrocyte morphology was changed in chronic colitis mouse brains compared with healthy mouse brains. In the brain of chronic colitis mice, astrocytes exhibited process extension, hypertrophy, and increased GFAP

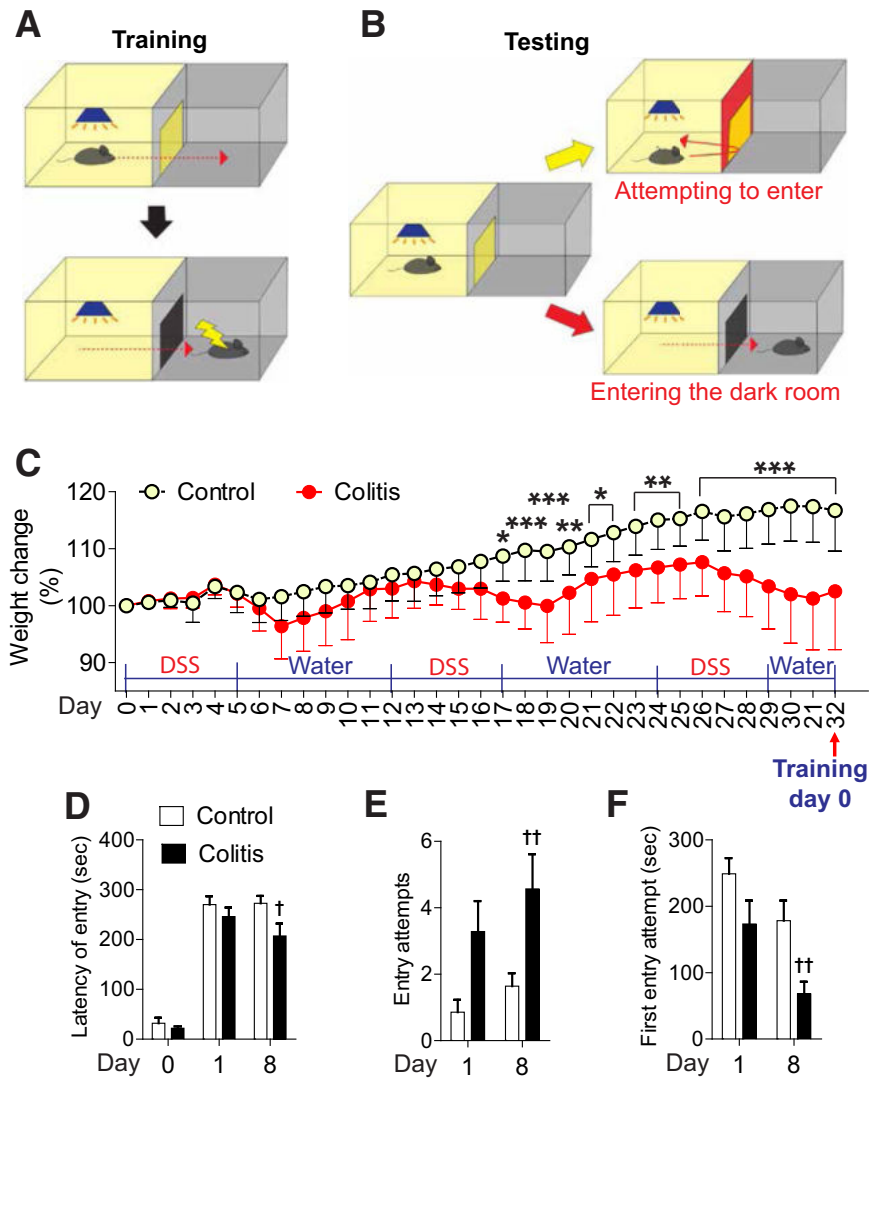


Figure 2 Chronic colitis mice have reduced long-term memory. To minimize potential effects in the brain due to hormonal variations, male C57BL/6 mice were used for the passive avoidance memory test. **A:** The illustration shows the training phase of the passive avoidance test. A mouse is placed in a lighted compartment. When the mouse follows its natural instinct to enter the dark compartment, the gate is closed quickly. Upon entering the dark room, the mouse experiences a mild electric shock to the paw. **B:** This illustration describes the testing phase. After being trained (**A**), the mouse is returned to the home cage for regular housing. One day later, the mouse is placed in the lighted room to test the time taken to enter the dark compartment; the result is quantified as a short-term memory measurement. The mouse is then returned to the home cage for regular housing for an additional 7 days. Next, it is again placed in the lighted room and subjected to the test. The data from day 8 are regarded as reflective of long-term memory. **C:** The chronic colitis C57BL/6 mice (8 weeks old; male) were treated with three cycles of dextran sulfate sodium (DSS) (2.5%) or water, followed by 3 days of water treatment for a brief recovery before testing. Body weight changes were evaluated from three independent experiments. **D–F:** Chronic colitis mice and healthy mice were trained in the passive avoidance apparatus (day 0). The short-term memory retention test was performed at twenty four hours while the long-term memory retention test was performed at eight days after training. The measurements indicate time taken by a mouse to enter the dark compartment (latency of entry) (**D**), the number of attempts to enter the dark room (**E**), and the time taken to first attempt to enter the dark room (**F**). Difference between colitis and control mice at each time point. Data were analyzed with the results obtained from three independent experiments. $n = 14$ per group (**C**, **E**, and **F**); $n = 21$ per group (**D**). $*P < 0.05$, $**P < 0.01$, $***P < 0.001$ versus control (two-way ANOVA, followed by the multiple-comparison Bonferroni t -test); $^{\dagger}P < 0.05$, $^{\dagger\dagger}P < 0.01$ versus control (U -test).

expression (Figure 3A), which are the phenotypic manifestations of reactive astrocytes. These results clearly show that chronic colitis induced reactive astrocytes in the mouse brain.

IL-1 β , IL-6, and IL-10 Levels Are Increased in the Hippocampus of Chronic Colitis Mice

Whether inflammatory mediators are up-regulated in the brain of the chronic colitis mice was examined next. IL-6 ($P < 0.001$) and IL-1 β ($P < 0.05$) levels increased in the hippocampus of the chronic colitis mice compared with the healthy mice (Figure 3B). However, the level of these inflammatory mediators was comparable in the cerebrum of these mouse groups. Immunofluorescence staining was used to further confirm that the positive staining of IL-1 β was

greatly increased in the hippocampal area of the chronic colitis mouse brain, as opposed to that in the control mouse brain (Figure 3C).

Elevated IL-10 levels have been reported in the brain of humans and rodents with neurodegenerative diseases^{34,35} and neuroinflammation.^{36,37} Given the role of IL-10 as a potent anti-inflammatory cytokine, increased IL-10 levels should be evolved to protect the brain from inflammation.³⁸

In line with these studies, IL-10 levels were substantially increased ($P < 0.001$) both in the hippocampus and in the cerebrum of the chronic colitis mice compared with negligible levels of IL-10 in the tissues of the control mice (Figure 3, D and E).

Whether acute colitis would result in the induction of inflammatory mediators in the brain was tested next. To address this, C57BL/6 mice were placed in a

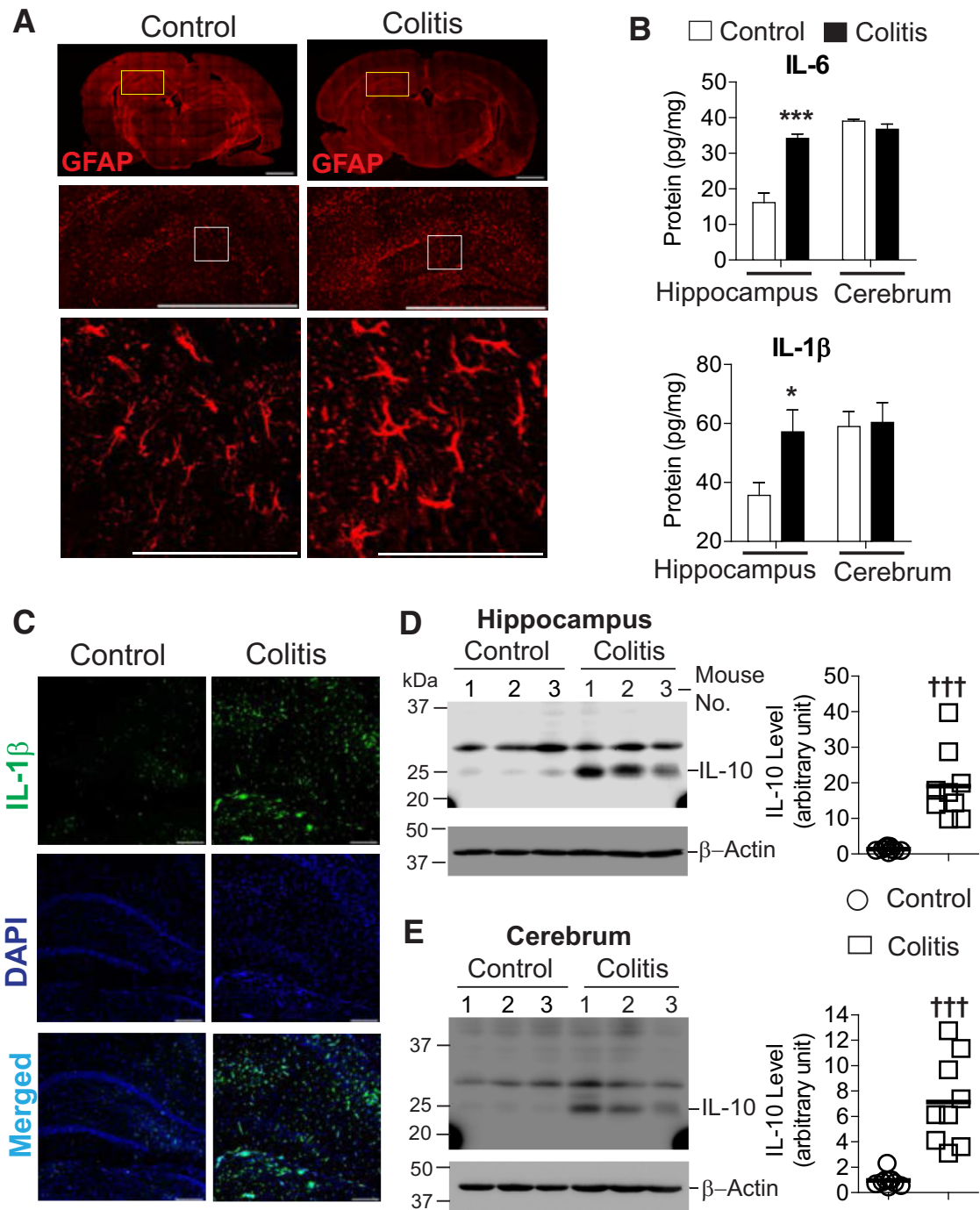


Figure 3 Chronic colitis mice exhibit neuroinflammation in the hippocampus. Sex-matched C57BL/6 (8 weeks old) mice were used. **A:** The brain sections from chronic colitis and control mice were subjected to immunofluorescence staining with the glial fibrillary acidic protein (GFAP) antibody. Confocal images were acquired by using a Zeiss LSM 800 confocal microscope and Zen 2 software. Tiles tool of the microscope was used to collect large tiled images of the GFAP staining, which are composed of a number of individual images. The **yellow boxed area** indicating the hippocampus is shown at higher magnification below. The **white boxed area** is shown at higher magnification below to examine the morphology of astrocytes. **B:** The hippocampus and cerebrum tissues were isolated from the mouse brain, followed by the preparation of the tissue lysates. IL-6 and IL-1 β levels were measured by using an enzyme-linked immunosorbent assay. Representative data are presented from three independent experiments. **C:** The mouse brain tissue sections were stained with an antibody recognizing IL-1 β , followed by fluorescein isothiocyanate-conjugated secondary antibody and DAPI staining. **D** and **E:** The hippocampus and cerebrum lysates were subjected to Western blot analysis to examine the level of IL-10 protein. β -actin was used as a loading control. Presented is the representative blot from three independent experiments. The density of the IL-10 band was quantified, and was normalized by that of β -actin (graphs at the right). Horizontal bar indicates a mean value. Immunofluorescence staining images presented are representative. Data are expressed as means \pm SEM (**B**). $n = 4$ per group, each with triplicate determinations (**B**); $n = 9$ per group (**D** and **E**). * $P < 0.05$, *** $P < 0.001$ versus control (one-tailed unpaired t -test); ††† $P < 0.001$ versus control (U -test). Scale bars: 1000 μ m (**A**, top row); 200 μ m (**A**, middle row, and **C**); and 25 μ m (**A**, bottom row).

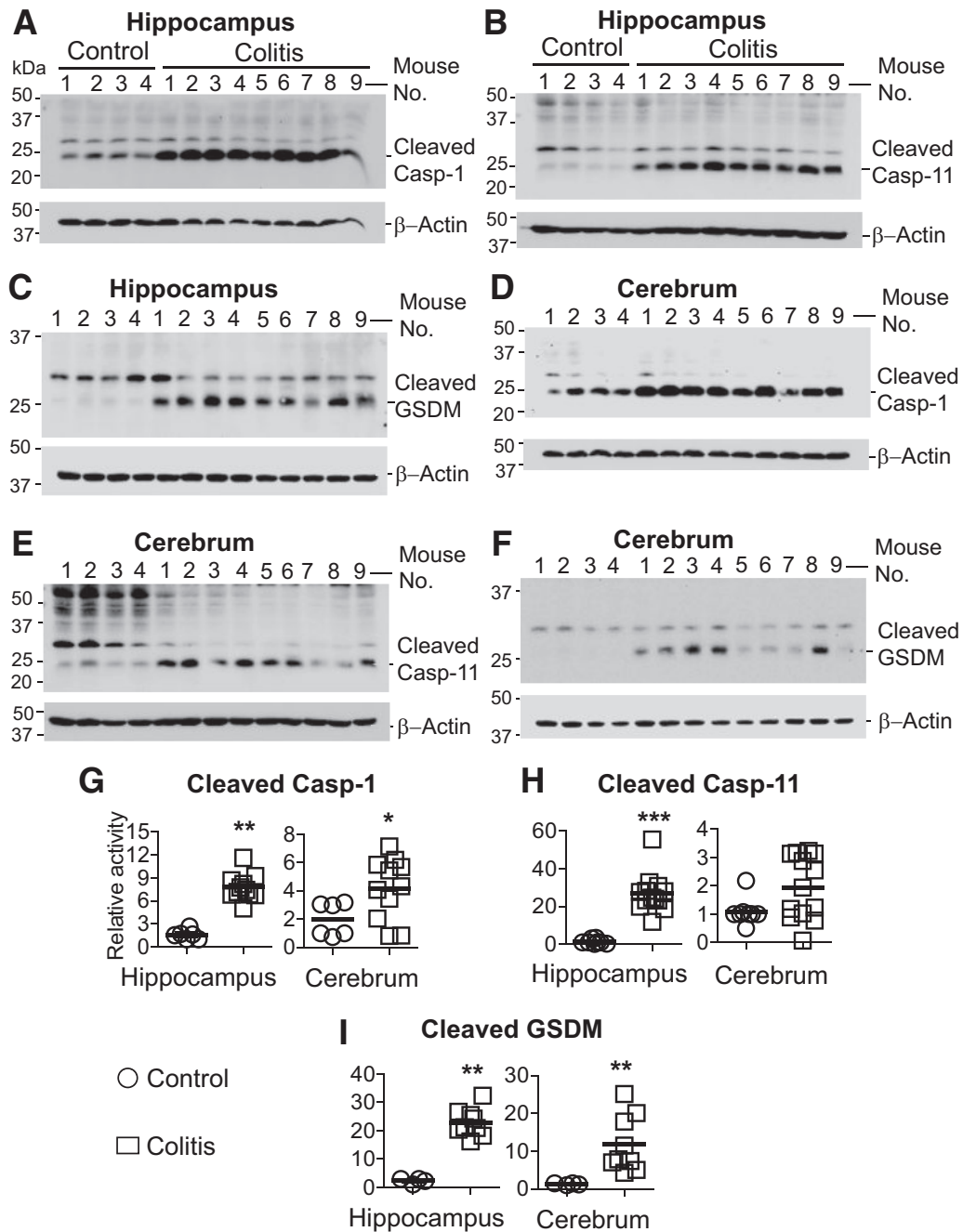


Figure 4 Caspase-1, caspase-11, and gasdermin (GSDM) are activated in the hippocampus of chronic colitis mice. Chronic colitis was induced in sex- and age-matched (8 weeks) C57BL/6 mice, followed by isolation of the hippocampus and cerebrum tissues. **A–F:** The tissue lysates were used for Western blot analysis with an antibody-recognizing cleaved caspase-1 (Casp-1), cleaved caspase-11 (Casp-11), or cleaved GSDM. β -actin was used as a loading control. **G–I:** We quantified the density of the band for cleaved Casp-1 (**G**), cleaved Casp-11 (**H**), and cleaved GSDM (**I**), which were normalized by that of β -actin. Horizontal bar indicates a mean value. Presented are the representative blots from two (Casp-1) or three (Casp-11) independent experiments. To avoid the protein aggregation that usually occurs in the Western blotting procedure, the heat denaturation (boiling) step was omitted^{26,27} before sample loading to SDS-PAGE. *n* = 6 controls (**G**); *n* = 11 colitis (**G**); *n* = 8 controls (**H**); *n* = 13 colitis (**H**); *n* = 4 controls (**I**); *n* = 9 colitis (**I**). **P* < 0.05, ***P* < 0.01, ****P* < 0.001 versus control (*U*-test).

single cycle of oral DSS (Supplemental Figure 2A). The production of inflammatory mediators (IL-1 β , IL-6, and tumor necrosis factor α) was up-regulated (*P* < 0.01) in the inflamed colon compared with those of control mice. However, levels of these

pro-inflammatory mediators were comparable in the brain tissues of the acute colitis and control mice (Supplemental Figure 2, B–D). These data suggest that acute colitis does not alter the level of inflammatory mediators in the brain.

Together, these results show that chronic colitis elicits inflammation in the brain.

Both Caspase-1 and Caspase-11 Are Activated in the Hippocampus of Chronic Colitis Mice

Activation of inflammatory receptors such as Toll-like receptors can up-regulate the level of pro-IL-1 β .³⁹ In parallel, inflammasome activation induces caspase-1 activation, which subsequently cleaves pro-IL-1 β protein to generate mature IL-1 β . The active form of caspase-1 further cleaves a family of gasdermin (GSDM) protein to liberate the N-terminal fragment of GSDM, which is oligomerized to create a pore-forming complex in the plasma membrane. This results in an inflammatory cell death termed pyroptosis. Conversely, caspase-11, a cytosolic LPS receptor,⁴⁰ is also able to activate a member of the GSDM family. In this way, caspase-11 activation also leads to pyroptosis.

Given the increased level of IL-1 β in the mouse hippocampus tissue, whether these cell death pathways could be activated in the brain tissue of chronic colitis mice was tested. Activation of caspase-1 ($P < 0.01$), caspase-11 ($P < 0.001$), and GSDM ($P < 0.01$) was greatly increased in the hippocampus tissues of the chronic colitis mice compared with that in the control mice (Figure 4, A–C, and G–I). Likewise, the activation of caspase-1 ($P < 0.05$) and GSDM ($P < 0.01$) was increased in the cerebrum tissues of the chronic colitis mice compared with that in the control mice (Figure 4, D and F). However, no noticeable difference was observed in caspase-11 activation in the cerebrum tissue of the chronic colitis mice compared with that in the control mice (Figure 4, E and H).

HMGB1 Levels Are Increased both in the Hippocampus and in the Serum of Chronic Colitis Mice

The mechanism by which chronic colitis may induce neuroinflammation was investigated next. Short-chain fatty acids are one of the main microbial metabolites and regulate an ascending connection between the gut and the brain.⁴¹ Moreover, reduced bacterial loads have been observed in the intestine of colitis mice.¹⁷ We therefore hypothesized that short-chain fatty acid concentrations might be changed in the brain of chronic colitis mice, which may reduce brain functionality. However, GC-MS analysis²⁴ found no difference in the short-chain fatty acid concentration between the hippocampus tissues of the chronic colitis mice and the control mice (Figure 5A).

Regarding the increased level of IL-1 β in the hippocampus of chronic colitis mice, IL-1 β production can be induced in macrophages stimulated by LPS.^{40,42} Accordingly, the amount of LPS was measured in the brain tissue from the chronic colitis mice and the control mice. However, these mice exhibited similar levels of LPS in their hippocampus and cerebrum tissues (Figure 5, B and C).

HMGB1 is a chromatin-binding nuclear protein⁴³ that can be secreted into the extracellular environment by necrotic or damaged cells and subsequently trigger a member of Toll-like receptors and the receptor for advanced glycation end-products, leading to activation of inflammatory responses, particularly in monocytes/macrophages.^{44,45} Furthermore, HMGB1 has the potential to induce the production of pro-IL-1 β in macrophages.⁴⁶ Elevated levels of HMGB1 protein have been observed in the stool of patients with IBD⁴⁷; immunohistochemical analysis has suggested increased HMGB1 in the colon tissue of DSS-induced colitis mice.⁴⁸ Therefore, we hypothesized that chronic inflammatory conditions in the gut liberate HMGB1 into extracellular regions, where it subsequently travels to the brain in which elevated levels of HMGB1 can induce neuroinflammation characterized by the induction of IL-1 β . To test this hypothesis, the level of HMGB1 in the mouse serum was evaluated. The concentration of HMGB1 was markedly increased in the serum of chronic colitis mice compared with that in control mice ($P < 0.001$) (Figure 5D), whereas serum LPS levels were similar between these groups (Figure 5E). Furthermore, considerably increased levels of HMGB1 were observed in the hippocampus tissue of chronic colitis mice compared with those of control mice ($P < 0.01$) (Figure 5F). However, the level of HMGB1 was comparable in the cerebrum of these mouse groups (Figure 5G).

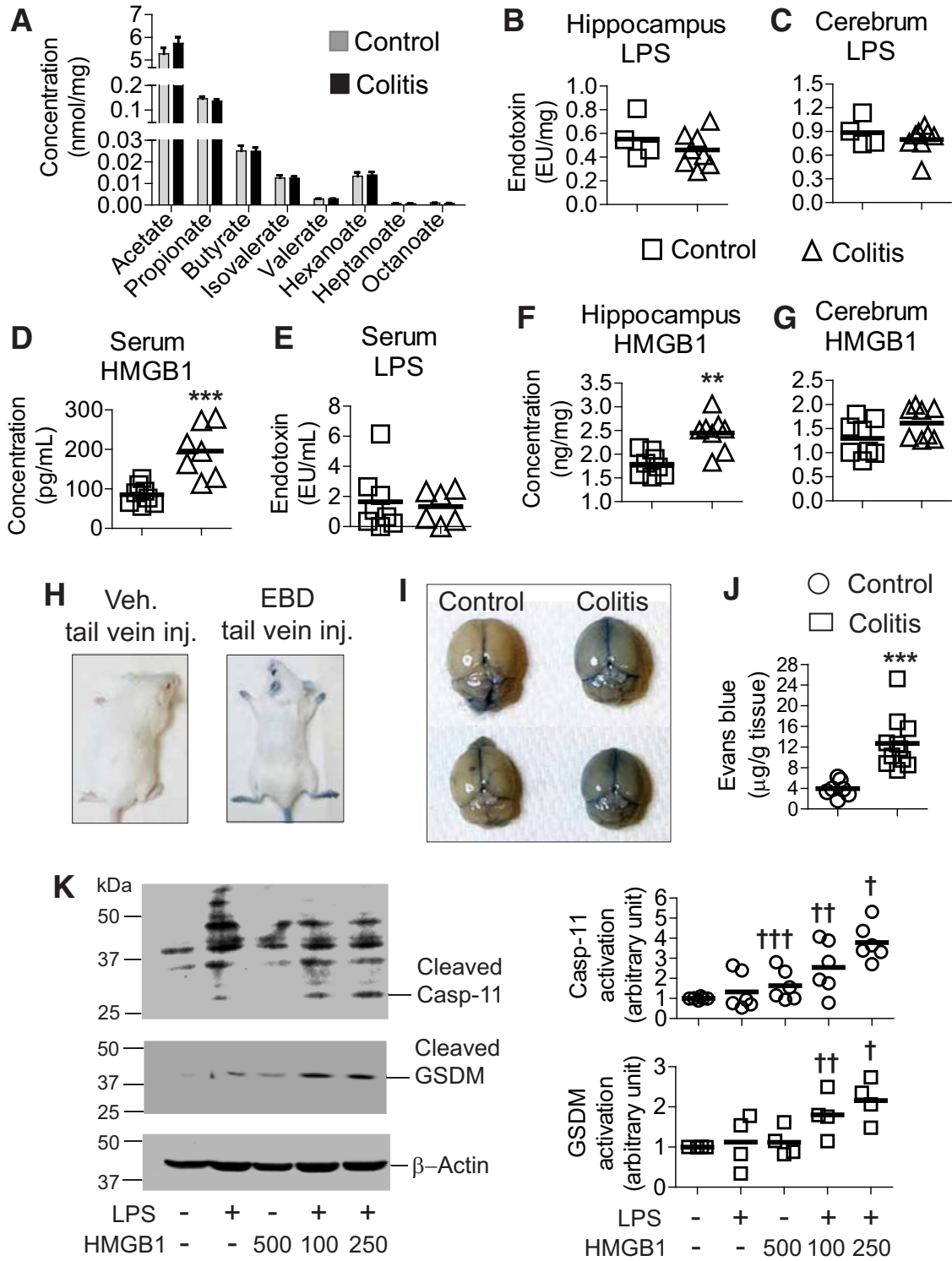
Together, these data suggest that mice with chronic colitis have elevated levels of HMGB1 both in the blood circulatory system and in the hippocampus.

Blood–Brain Barrier Permeability Is Increased in Chronic Colitis Mice

Given the increased level of HMGB1 both in the hippocampus and in the blood, we next hypothesized that chronic colitis would result in a leaky blood–brain barrier (BBB); thereby, extracellular HMGB1 protein could be translocated from the blood circulatory system to the brain. To test this hypothesis, the BBB permeability was examined using tail vein administration of EBD. Higher levels of EBD were observed in the brain of the chronic colitis mice compared with the control mouse brains (Figure 5, H–J). Thus, these data indicate that the BBB permeability is increased in chronic colitis mice.

In the Presence of LPS, HMGB1 Activates the Caspase-11–Mediated Pyroptosis Pathway in Microglial Cells

Caspase-1 and caspase-11 can be activated in monocytes/macrophages, leading to IL-1 β secretion and pyroptosis. HMGB1 itself can stimulate macrophages to elicit inflammatory responses. Therefore, microglia, which are central nervous system–resident macrophages, likely have an important role in the induction of neuroinflammation in chronic colitis mice. Intriguingly, a recent study suggested



that HMGB1 can function as an LPS transporter that delivers extracellular LPS into the cytosol, where it consequently activates the cytosolic LPS receptor caspase-11 and subsequently cleaves GSDM to cause pyroptosis in macrophages.⁴⁹ Along this line, we hypothesized that increased HMGB1 in the hippocampus could be associated with neuroinflammation in chronic colitis mice.

To test this hypothesis, whether HMGB1 stimulation in the mouse microglial cell line SIM-A9 activates caspases was examined. The treatment of HMGB1 alone was able to induce moderate activation of caspase-11 in microglial cells; however, GSDM activation was not induced (Figure 5K). This result suggests that HMGB1 alone may not be sufficient to induce inflammatory responses in microglial cells. Given the elevated HMGB1 levels and unchanged LPS levels in the brain tissues of chronic colitis mice, SIM-A9 cells were next co-treated with HMGB1 protein and LPS. In the presence of LPS, HMGB1 potently activated both caspase-11 and GSDM in microglial cells.

These data suggest that increased levels of HMGB1 in conjunction with LPS are capable of potently activating both caspase-11 and GSDM to induce microglial cell pyroptosis.

Discussion

IBD is a chronic inflammatory disorder in the gastrointestinal tract caused by abnormal immune responses to commensal microbes in genetically susceptible individuals.^{50,51} Many patients with IBD also develop extraintestinal manifestations in the skin, joints, eyes, and liver.⁵² A longitudinal cohort study with patients with IBD recently identified that the incidence of dementia, including Alzheimer disease, is four times higher in patients with

ulcerative colitis and CD than in non-IBD control patients, with no sex differences.⁵³ Other cohort studies suggest that IBD may increase the risk of Parkinson disease.^{54,55}

In an effort to elucidate a potential mechanism by which IBD increases the risk of neurodegenerative diseases, neurodegenerative disease—causing α -synuclein and Tau proteins⁵⁶ were examined in the colon of patients with IBD. For instance, elevated Tau protein was reported in the colon biopsy sample of CD but not in ulcerative colitis; decreased mechanism of protein clearance might result in this accumulation.⁵⁷ Nonetheless, direct evidence for and an underlying mechanism of this interplay between the inflamed gut and the brain remain elusive.

The present study showed that chronic colitis suppresses the functional activity of the mouse hippocampus. Furthermore, it suggests HMGB1 as a key molecule that can mediate neuroinflammatory responses in chronic colitis mice. As a damage-associated molecular pattern secreted to an extracellular environment, HMGB1 activates specific receptors to induce inflammatory responses, primarily in monocytes/macrophages. Thus, HMGB1 liberated from inflamed tissues can induce a second wave of inflammation in peripheral tissues. Elevated HMGB1 levels have been identified in the intestine of patients with IBD.⁴⁷ Similarly, the current data show that HMGB1 levels are markedly increased both in the blood circulatory system and in the hippocampus of chronic colitis mice. Regarding the elevated HMGB1 protein level in the hippocampus of the chronic colitis mice, it should be taken into account that trinitrobenzene sulfonic acid—induced colitis in rabbits increases the BBB permeability,⁵⁸ and systemic inflammation may increase the BBB permeability in humans.⁵⁹ BBB permeability was increased in DSS-induced chronic colitis mice, corroborating the above observations (Figure 5, H–J).

Figure 5 High-mobility group box 1 (HMGB1) is involved in the activation of neuroinflammation in chronic colitis mice. **A–G:** From sex-matched and age-matched (8 weeks) chronic colitis or healthy C57BL/6 mice, the hippocampus and cerebrum tissues were harvested without perfusion. Using gas chromatography–mass spectrometry analysis, short-chain fatty acid concentrations of the tissues were quantified (**A**). The tissue lysates were used for the endotoxin assay in the control mice and chronic colitis mice (**B** and **C**). Blood serum samples were collected from chronic colitis mice and control mice, and then subjected to the HMGB1 enzyme-linked immunosorbent assay and the endotoxin assay (**D** and **E**). The tissue lysates were used for the HMGB1 enzyme-linked immunosorbent assay in the chronic colitis mice and control mice (**F** and **G**). Representative data (**B–F**) are presented from more than two independent experiments. **H–J:** To examine the blood–brain barrier permeability, sex-/age-matched CD-1 mice (white coat color) were used because a successful tail vein injection (inj.) of Evans blue dye (EBD) can be easily verified due to its white coat color. When mice are tail vein injected with vehicle (Veh.) or EBD (2%), a successful tail vein injection immediately turns the limb and ear blue. This is an indicator of a successful tail vein injection (**H**). CD-1 mice were treated with three cycles of dextran sulfate sodium (2.5%) for chronic colitis or with water for controls. After finishing the third dextran sulfate sodium cycle, mice were tail vein injected with EBD. One hour after the injection, mice were anesthetized with isoflurane and transcardially perfused with 0.9% NaCl saline. The brain was harvested (**I**). The brains were then dried at 60°C for 48 hours. EBD was extracted in 0.5 mL formamide at room temperature for 48 hours. EBD was quantified by spectrofluorimetry (excitation, 620 nm; emission, 680 nm). Data are normalized to the brain weight. Combined data from 2 different experiments are presented (**J**). **K:** Mouse microglial cell line SIM-A9 cells were treated with various concentrations of HMGB1 (in nanograms per milliliter) with or without lipopolysaccharide (LPS) (1 μ g/mL) for 24 hours. The activation of caspase-11 and gasdermin (GSDM) was assessed through Western blotting in which the sample boiling step was omitted to prevent protein aggregation (**left panels**). The density of the band for cleaved caspase-11 and cleaved GSDM was quantified, and was normalized to β -actin (**right panels**). Representative blot of four or six independent experiments is presented. The data of each group were compared with those of vehicle-treated group. Horizontal bar in graphs indicates a mean value. $n = 8$ per group (**A**); $n = 4$ control mice (**B** and **C**); $n = 8$ chronic colitis mice (**B** and **C**); $n = 7$ chronic colitis mice (**D** and **E**); $n = 8$ control mice (**D** and **E**); $n = 8$ chronic colitis mice (**F** and **G**); $n = 8$ control mice (**F** and **G**); $n = 7$ control mice (**J**); $n = 11$ chronic colitis mice (**J**). * $P < 0.05$, ** $P < 0.01$, *** $P < 0.001$ versus control (*U*-test); † $P < 0.05$, †† $P < 0.01$, ††† $P < 0.001$ versus untreated control (one-tailed unpaired *t*-test).

The hippocampus is perfused by branches of multiple blood vessels, including the posterior cerebral artery, the anterior choroidal artery, and numerous internal hippocampal arterioles.⁶⁰ An elegant study by Mazarati et al⁶¹ suggested that HMGB1 can impair memory in mice through both Toll-like receptor 4 and the receptor for advanced glycation end-products. It is therefore reasonable to believe that HMGB1 from the inflamed colon migrated through the blood circulatory system and then traveled into the hippocampus of the chronic colitis mice through the compromised BBB.

Regarding the molecular mechanism by which HMGB1 may induce neuroinflammation, the study suggests that augmented HMGB1, in conjunction with a low level of indigenous LPS, is capable of activating caspases in the hippocampus to induce neuroinflammatory responses. Indeed, this was confirmed by co-stimulation of HMGB1 together with LPS induces potent activation of caspase-11 and GSDM in mouse microglial cells. However, the stimulation of either HMGB1 or LPS alone is not sufficient to elicit the inflammatory response in microglial cells. This finding is in agreement with the study indicating that HMGB1 transports LPS from extracellular regions into the cytosol, and LPS can then activate caspase-11 to induce pyroptosis.⁴⁹ It is thus reasonable to believe that HMGB1 plays an essential role in inducing the activation of caspase-11 and GSDM in microglial cells.

It is worth noting that the concentration of LPS and HMGB1 used to simulate SIM-A9 cells is higher than the concentration observed in the brain tissue. This discrepancy may be due to the different experimental systems: *in vivo* mouse experiments versus *in vitro* experiments with a cell line. For the *in vitro* experiment, an immortalized mouse microglial cell line was used, which may be less sensitive to extracellular stimulatory factors than resident microglia of the brain. It is therefore reasonable to believe that relatively high doses of LPS and HMGB1 would be applied for *in vitro* experiments to elicit potent cellular responses when recapitulating *in vivo* physiological changes.

Both caspase-1 and caspase-11 activation was observed in the hippocampus of chronic colitis mice, wherein HMGB1 levels were elevated. In contrast, caspase-11 activation, but not caspase-1 activation, was observed in microglial cells. To explain this difference, it should be taken into account that elevated HMGB1 levels transport LPS into the cytosolic region of microglia, followed by the activation of caspase-11 to induce pyroptosis. This inflammatory cell death results in releasing endogenous danger signals such as ATP and reactive oxygen species. These signals then mediate canonical inflammasome activation to activate caspase-1, resulting in pro-IL-1 β maturation and GSDM activation to induce pyroptosis. In this way, HMGB1 may also have the potential to activate caspase-1 in an *in vivo* condition.⁶²

Intriguingly, IL-1 β levels and caspase-11 activation were not altered in the cerebrum tissues of chronic colitis and

control mice (Figures 3B and 4H). Moreover, the degree of caspase-1 activation in the cerebrum of chronic colitis mice was relatively low compared with the potent activation in the hippocampus (Figure 4G). Considering these data, we speculate that the hippocampus is more sensitive to the chronic colitis condition than the cerebrum. To explain this, the distribution of microglia should be considered. Microglia reside throughout all major anatomic regions of the brain but are variably distributed across these regions. A large number of microglia reside in the hippocampus, whereas their population is low in the cerebrum.⁶³ Moreover, the activation of caspase-1 and caspase-11, and consequent IL-1 β production and pyroptosis, occurs primarily in monocytes/macrophages. Therefore, the high population of microglia in the hippocampus likely helps to explain why inflammatory responses are strongly elicited in the hippocampus but far less strongly induced in the cerebrum.

Thus, the multi-cycle DSS treatment^{11,16} was harnessed as a model of chronic colitis, in which colitis development depends on epithelial injury caused by oral consumption of DSS-containing water.³⁰ It is worth noting that DSS is not detected in the brain of DSS-induced colitis mice,⁶⁴ suggesting that DSS does not migrate to the brain to induce any pathologic effects.

In summary, this study provides direct evidence for the ascending connection between the inflamed gut and the brain but also suggests the pathway of HMGB1-associated pyroptosis as an underlying mechanism.

Acknowledgments

We thank the team of Metabolomics Core Services at the University of Michigan, Ann Arbor, for the GC-MS and data analysis; and Dr. Bruce Berkowitz, Dr. Yimin Shen, and Robin Roberts at the MR Core Research Facility, Wayne State University, for the mouse MEMRI.

Supplemental Data

Supplemental material for this article can be found at <http://doi.org/10.1016/j.ajpath.2021.09.006>.

Author Contributions

S.H.R. and E.I. conceived and designed the experiments; S.H.R. and J.M. performed the MRI experiments; S.H.R. and E.I. analyzed the MRI data; S.L., J.Y.H., and J.L. conducted the passive avoidance test and ELISA; S.J.K. performed ELISA, immunofluorescence staining, and immunoblotting experiments; J.M., C.H., and M.P. performed ELISA and immunoblotting experiments; S.H.R. and E.I. wrote the paper.

References

- Rhee SH, Pothoulakis C, Mayer EA: Principles and clinical implications of the brain-gut-enteric microbiota axis. *Nat Rev Gastroenterol Hepatol* 2009, 6:306–314
- Jones MP, Dillely JB, Drossman D, Crowell MD: Brain-gut connections in functional GI disorders: anatomic and physiological relationships. *Neurogastroenterol Motil* 2006, 18:91–103
- Levenstein S, Prantera C, Varvo V, Scribano ML, Andreoli A, Luzzi C, Arcà M, Berto E, Milite G, Marcheggiano A: Stress and exacerbation in ulcerative colitis: a prospective study of patients enrolled in remission. *Am J Gastroenterol* 2000, 95:1213–1220
- Meddings JB, Swain MG: Environmental stress-induced gastrointestinal permeability is mediated by endogenous glucocorticoids in the rat. *Gastroenterology* 2000, 119:1019–1028
- Killinger BA, Madaj Z, Sikora JW, Rey N, Haas AJ, Vepa Y, Lindqvist D, Chen H, Thomas PM, Brundin P, Brundin L, Labrie V: The vermiform appendix impacts the risk of developing Parkinson's disease. *Sci Transl Med* 2018, 10:eaar5280
- Kristensen VA, Valeur J, Brackmann S, Jahnson J, Brunborg C, Tveito K: Attention deficit and hyperactivity disorder symptoms respond to gluten-free diet in patients with coeliac disease. *Scand J Gastroenterol* 2019, 54:571–576
- Yelland GW: Gluten-induced cognitive impairment (“brain fog”) in coeliac disease. *J Gastroenterol Hepatol* 2017, 32(Suppl):90–93
- Petruo VA, Zeissig S, Schmelz R, Hampe J, Beste C: Specific neurophysiological mechanisms underlie cognitive inflexibility in inflammatory bowel disease. *Sci Rep* 2017, 7:13943
- Gracie DJ, Guthrie EA, Hamlin PJ, Ford AC: Bi-directionality of brain-gut interactions in patients with inflammatory bowel disease. *Gastroenterology* 2018, 154:1635–1646.e3
- Kurina LM, Goldacre MJ, Yeates D, Gill LE: Depression and anxiety in people with inflammatory bowel disease. *J Epidemiol Community Health* 2001, 55:716–720
- Zonis S, Pechnick RN, Ljubimov VA, Mahgerefteh M, Wawrowsky K, Michelsen KS, Chesnokova V: Chronic intestinal inflammation alters hippocampal neurogenesis. *J Neuroinflammation* 2015, 12:65
- Lauterbur PC: Image formation by induced local interactions—examples employing nuclear magnetic-resonance. *Nature* 1973, 242:190–191
- Malheiros JM, Paiva FF, Longo BM, Hamani C, Covolan L: Manganese-enhanced MRI: biological applications in neuroscience. *Front Neurol* 2015, 6:161
- Takeda A: Manganese action in brain function. *Brain Res Brain Res Rev* 2003, 41:79–87
- Lin YJ, Koretsky AP: Manganese ion enhances T1-weighted MRI during brain activation: an approach to direct imaging of brain function. *Magn Reson Med* 1997, 38:378–388
- Takedatsu H, Michelsen KS, Wei B, Landers CJ, Thomas LS, Dhall D, Braun J, Targan SR: TL1A (TNFSF15) regulates the development of chronic colitis by modulating both T-helper 1 and T-helper 17 activation. *Gastroenterology* 2008, 135:552–567
- Im E, Jung J, Pothoulakis C, Rhee SH: Disruption of Pten speeds onset and increases severity of spontaneous colitis in *il10*($-/-$) mice. *Gastroenterology* 2014, 147:667–679.e10
- Berkowitz BA, Bissig D, Patel P, Bhatia A, Roberts R: Acute systemic 11-cis-retinal intervention improves abnormal outer retinal ion channel closure in diabetic mice. *Mol Vis* 2012, 18:372–376
- Chuang K-H, Koretsky AP, Sotak CH: Temporal changes in the T1 and T2 relaxation rates (DeltaR1 and DeltaR2) in the rat brain are consistent with the tissue-clearance rates of elemental manganese. *Magn Reson Med* 2009, 61:1528–1532
- Saria A, Lundberg JM: Evans blue fluorescence: quantitative and morphological evaluation of vascular permeability in animal tissues. *J Neurosci Methods* 1983, 8:41–49
- Emanuelli C, Grady EF, Madeddu P, Figini M, Bunnett NW, Parisi D, Regoli D, Geppetti P: Acute ACE inhibition causes plasma extravasation in mice that is mediated by bradykinin and substance P. *Hypertension* 1998, 31:1299–1304
- Tucker AR, Gibbs ME, Stanes MD: Cycloheximide and passive avoidance memory in mice: time-response, dose-response and short-term memory. *Pharmacol Biochem Behav* 1976, 4:441–446
- Oh SB, Park HR, Jang YJ, Choi SY, Son TG, Lee J: Baicalein attenuates impaired hippocampal neurogenesis and the neurocognitive deficits induced by [gamma]-ray radiation. *Br J Pharmacol* 2013, 168:421–431
- Lorenz MA, Burant CF, Kennedy RT: Reducing time and increasing sensitivity in sample preparation for adherent mammalian cell metabolomics. *Anal Chem* 2011, 83:3406–3414
- Nagamoto-Combs K, Kulas J, Combs CK: A novel cell line from spontaneously immortalized murine microglia. *J Neurosci Methods* 2014, 233:187–198
- Gallagher SR, Leonard RT: Electrophoretic characterization of a detergent-treated plasma membrane fraction from corn roots. *Plant Physiol* 1987, 83:265–271
- McLane MW, Hatzidimitriou G, Yuan J, McCann U, Ricaurte G: Heating induces aggregation and decreases detection of serotonin transporter protein on western blots. *Synapse* 2007, 61:875–876
- Mitchell J, Kim SJ, Seelmann A, Veit B, Shepard B, Im E, Rhee SH: Src family kinase tyrosine phosphorylates Toll-like receptor 4 to dissociate MyD88 and Mal/Tirap, suppressing LPS-induced inflammatory responses. *Biochem Pharmacol* 2018, 147:119–127
- Kim SJ, Howe C, Mitchell J, Choo J, Powers A, Oikonomopoulos A, Pothoulakis C, Hommes DW, Im E, Rhee SH: Autotaxin loss accelerates intestinal inflammation by suppressing TLR4-mediated immune responses. *EMBO Rep* 2020, 21:e49332
- Okayasu I, Hatakeyama S, Yamada M, Ohkusa T, Inagaki Y, Nakaya R: A novel method in the induction of reliable experimental acute and chronic ulcerative colitis in mice. *Gastroenterology* 1990, 98:694–702
- Pekny M, Pekna M: Reactive gliosis in the pathogenesis of CNS diseases. *Biochim Biophys Acta* 2016, 1862:483–491
- Liesi P, Kaakkola S, Dahl D, Vaehri A: Laminin is induced in astrocytes of adult brain by injury. *EMBO J* 1984, 3:683–686
- Saha P, Sarkar S, Ramesh Kumar P, Biswas SC: TIMP-1: a key cytokine released from activated astrocytes protects neurons and ameliorates cognitive behaviours in a rodent model of Alzheimer's disease. *Brain Behav Immun* 2020, 87:804–819
- Apelt J, Schliebs R: Beta-amyloid-induced glial expression of both pro- and anti-inflammatory cytokines in cerebral cortex of aged transgenic Tg2576 mice with Alzheimer plaque pathology. *Brain Res* 2001, 894:21–30
- Rentzos M, Nikolaou C, Andreadou E, Paraskevas GP, Rombos A, Zoga M, Tsoutsou A, Boufidou F, Kapaki E, Vassilopoulos D: Circulating interleukin-10 and interleukin-12 in Parkinson's disease. *Acta Neurol Scand* 2009, 119:332–337
- Jander S, Pohl J, D'Urso D, Gillen C, Stoll G: Time course and cellular localization of interleukin-10 mRNA and protein expression in autoimmune inflammation of the rat central nervous system. *Am J Pathol* 1998, 152:975–982
- Hulshof S, Montagne L, De Groot CJA, Van Der Valk P: Cellular localization and expression patterns of interleukin-10, interleukin-4, and their receptors in multiple sclerosis lesions. *Glia* 2002, 38:24–35
- Lobo-Silva D, Carriche GM, Castro AG, Roque S, Saraiva M: Balancing the immune response in the brain: IL-10 and its regulation. *J Neuroinflammation* 2016, 13:297
- Kayagaki N, Warming S, Lamkanfi M, Vande Walle L, Louie S, Dong J, Newton K, Qu Y, Liu J, Heldens S, Zhang J, Lee WP, Roose-Girma M, Dixit VM: Non-canonical inflammasome activation targets caspase-11. *Nature* 2011, 479:117–121

40. Shi J, Zhao Y, Wang Y, Gao W, Ding J, Li P, Hu L, Shao F: Inflammatory caspases are innate immune receptors for intracellular LPS. *Nature* 2014, 514:187–192
41. Li Z, Yi C-X, Katiraei S, Kooijman S, Zhou E, Chung CK, Gao Y, van den Heuvel JK, Meijer OC, Berbée JFP, Heijink M, Giera M, Willems van Dijk K, Groen AK, Rensen PCN, Wang Y: Butyrate reduces appetite and activates brown adipose tissue via the gut-brain neural circuit. *Gut* 2018, 67:1269–1279
42. Zanoni I, Tan Y, Di Gioia M, Broggi A, Ruan J, Shi J, Donado CA, Shao F, Wu H, Springstead JR, Kagan JC: An endogenous caspase-11 ligand elicits interleukin-1 release from living dendritic cells. *Science* 2016, 352:1232–1236
43. Goodwin GH, Sanders C, Johns EW: A new group of chromatin-associated proteins with a high content of acidic and basic amino acids. *Eur J Biochem* 1973, 38:14–19
44. Andersson U, Wang H, Palmblad K, Aveberger AC, Bloom O, Erlandsson-Harris H, Janson A, Kokkola R, Zhang M, Yang H, Tracey KJ: High mobility group 1 protein (HMG-1) stimulates proinflammatory cytokine synthesis in human monocytes. *J Exp Med* 2000, 192:565–570
45. Scaffidi P, Misteli T, Bianchi ME: Release of chromatin protein HMGB1 by necrotic cells triggers inflammation. *Nature* 2002, 418:191–195
46. He Q, You H, Li X-M, Liu T-H, Wang P, Wang B-E: HMGB1 promotes the synthesis of pro-IL-1[β] and pro-IL-18 by activation of p38 MAPK and NF- κ B through receptors for advanced glycation end-products in macrophages. *Asian Pac J Cancer Prev* 2012, 13:1365–1370
47. Vitali R, Stronati L, Negroni A, Di Nardo G, Pierdomenico M, del Giudice E, Rossi P, Cucchiara S: Fecal HMGB1 is a novel marker of intestinal mucosal inflammation in pediatric inflammatory bowel disease. *Am J Gastroenterol* 2011, 106:2029–2040
48. Yamasaki H, Mitsuyama K, Masuda J, Kuwaki K, Takedatsu H, Sugiyama G, Yamada S, Sata M: Roles of high-mobility group box 1 in murine experimental colitis. *Mol Med Rep* 2009, 2:23–27
49. Deng M, Tang Y, Li W, Wang X, Zhang R, Zhang X, Zhao X, Liu J, Tang C, Liu Z, Huang Y, Peng H, Xiao L, Tang D, Scott MJ, Wang Q, Liu J, Xiao X, Watkins S, Li J, Yang H, Wang H, Chen F, Tracey KJ, Billiar TR, Lu B: The endotoxin delivery protein HMGB1 mediates caspase-11-dependent lethality in sepsis. *Immunity* 2018, 49:740–753.e7
50. Mitchell J, Kim SJ, Koukos G, Seelmann A, Veit B, Shepard B, Blumer-Schuette S, Winter HS, Iliopoulos D, Pothoulakis C, Im E, Rhee SH: Colonic inhibition of phosphatase and tensin homolog increases colitogenic bacteria, causing development of colitis in *Il10*^{-/-} mice. *Inflamm Bowel Dis* 2018, 24:1718–1732
51. Yan J, Hedl M, Abraham C: An inflammatory bowel disease-risk variant in INAVA decreases pattern recognition receptor-induced outcomes. *J Clin Invest* 2017, 127:2192–2205
52. Vavricka SR, Schoepfer A, Scharl M, Lakatos PL, Navarini A, Rogler G: Extraintestinal manifestations of inflammatory bowel disease. *Inflamm Bowel Dis* 2015, 21:1982–1992
53. Zhang B, Wang HE, Bai Y-M, Tsai S-J, Su T-P, Chen T-J, Wang Y-P, Chen M-H: Inflammatory bowel disease is associated with higher dementia risk: a nationwide longitudinal study. *Gut* 2020, 70:85–91
54. Lin J-C, Lin C-S, Hsu C-W, Lin C-L, Kao C-H: Association between Parkinson's disease and inflammatory bowel disease: a nationwide Taiwanese retrospective cohort study. *Inflamm Bowel Dis* 2016, 22:1049–1055
55. Villumsen M, Aznar S, Pakkenberg B, Jess T, Brudek T: Inflammatory bowel disease increases the risk of Parkinson's disease: a Danish nationwide cohort study 1977-2014. *Gut* 2019, 68:18–24
56. Moussaud S, Jones DR, Moussaud-Lamodière EL, Delenclos M, Ross OA, McLean PJ: Alpha-synuclein and tau: teammates in neurodegeneration? *Mol Neurodegener* 2014, 9:43
57. Prigent A, Chapelet G, De Guilhem de Lataillade A, Oullier T, Durieu E, Bourreille A, Duchalais E, Hardonnière K, Neunlist M, Noble W, Kerdine-Römer S, Derkinderen P, Rolli-Derkinderen M: Tau accumulates in Crohn's disease gut. *FASEB J* 2020, 34:9285–9296
58. Hathaway CA, Appleyard CB, Percy WH, Williams JL: Experimental colitis increases blood-brain barrier permeability in rabbits. *Am J Phys* 1999, 276:G1174–G1180
59. Varatharaj A, Galea I: The blood-brain barrier in systemic inflammation. *Brain Behav Immun* 2017, 60:1–12
60. Rusinek H, Brys M, Glodzik L, Switalski R, Tsui W-H, Haas F, McGorty K, Chen Q, de Leon MJ: Hippocampal blood flow in normal aging measured with arterial spin labeling at 3T. *Magn Reson Med* 2011, 65:128–137
61. Mazarati A, Maroso M, Iori V, Vezzani A, Carli M: High-mobility group box-1 impairs memory in mice through both toll-like receptor 4 and receptor for advanced glycation end products. *Exp Neurol* 2011, 232:143–148
62. Yan W, Chang Y, Liang X, Cardinal JS, Huang H, Thorne SH, Monga SPS, Geller DA, Lotze MT, Tsung A: High-mobility group box 1 activates caspase-1 and promotes hepatocellular carcinoma invasiveness and metastases. *Hepatology* 2012, 55:1863–1875
63. Lawson LJ, Perry VH, Dri P, Gordon S: Heterogeneity in the distribution and morphology of microglia in the normal adult mouse brain. *Neuroscience* 1990, 39:151–170
64. Kitajima S, Takuma S, Morimoto M: Tissue distribution of dextran sulfate sodium (DSS) in the acute phase of murine DSS-induced colitis. *J Vet Med Sci* 1999, 61:67–70